

Characterization of 3D integrated APS for X-ray detection.

G. Prigozhin¹, V. Suntharalingam², D. Busacker², R. Foster¹, S. Kissel¹, B. LaMarr¹, A. Soares², M. Bautz¹

¹*Kavli Institute for Astrophysics and Space Research, Massachusetts Institute of Technology*

²*Lincoln Laboratory, Massachusetts Institute of Technology*

Active Pixel Sensors are being developed for a rapidly growing number of imaging applications in response to dramatic improvements in sensor performance. One area where development seems to be less intense is direct detection of low energy X-rays, an application that is vital for high energy astrophysics, and at the moment is entirely dominated by CCDs. X-ray detectors for scientific applications differ from commercial visible sensors in several respects. They require much thicker photo-sensitive volume because X-rays in this band are more penetrating. Excellent charge collection efficiency is required for good X-ray spectroscopic performance, and this implies that photo-sensitive volume must be fully depleted. Good X-ray detection efficiency requires back illumination, since refractive optics cannot be used to compensate for the lower fill-factor of FI devices. Very low read noise is essential to measure very small charge packets (of order 10^2 to 10^3 electrons) deposited by X-ray photons.

Here we describe results of a new approach where a sensor was built using 3D integration technology developed at MIT Lincoln Laboratory. A silicon diode array is fabricated in one wafer (or 'tier') and then integrated with CMOS readout circuitry on a separate SOI wafer from which the substrate has been removed. This scheme allows much tighter integration than other hybrid technologies, and, since more than two tiers can be stacked together, its signal processing capabilities are almost limitless. An SEM photograph of the pixel cross section depicting readout circuit tier and a portion of thick detector tier is shown in Fig. 1. Tungsten plugs that connect them are clearly visible.

The device is an array of 256 x 256 pixels with a pixel size of 24 x 24 microns, typical for scientific X-ray sensors. The photodiode tier is 50 microns thick and in order to be fully depletable it is made on a high resistivity 3000 Ohm-cm n-type substrate. SOI readout is fabricated in a 0.35 μm technology with 3.3V operating voltage. The device schematic is shown in Fig. 2. Pixel includes two stages separated by a large 787 fF capacitor C_1 , which is introduced to do in-pixel reset noise subtraction. Having advantages of SOI technology, we used p-channel transistors as reset switches, thus avoiding the problem of dealing with "soft reset" lag.

In order to investigate what are the sources of noise contributing to the signal, we implemented a readout mode in which a single pixel was readout multiple times after being reset only once. In such a mode reset noise can be easily eliminated. Fig. 3Left shows signal as a function of time during a full period from one reset pulse to another and containing an X-ray event.

Fig. 3Right shows a histogram of the X-ray events accumulated when the chip was illuminated by ^{55}Fe radioactive source. Characteristic lines of Mn at 5.89 and 6.4 keV are very well resolved. The energy resolution of K_{α} line of 181 eV is close to the Fano limited resolution of 162 eV for the corresponding readout noise level of 12.6 electrons, clearly indicating that charge collection efficiency is very high. This is especially remarkable since this is a histogram of all events exceeding certain threshold; no selection of events has been made based on the analysis of the signal amplitude in the adjacent pixels, and such selection tends to improve energy resolution. Once the X-ray peak is found, it is easy to determine the responsivity and the sense node capacitance, which were calculated to be, respectively, 4.6 $\mu\text{V}/\text{electron}$ and 24.7 fF.

The sense node capacitance includes two components connected in parallel: the input capacitance of the readout circuit and the capacitance of the charge collecting photodiode. The capacitance of photodiode is a strong function of the voltage applied to the p-n junction, while the circuit capacitance is decoupled from it. This presents a way to separate contributions of these components by varying voltage applied to the photodiode. The result of such measurement is shown in Fig. 4. The data points were approximated by an analytical expression describing capacitance of the linearly graded junction, the best fit produced the value of the circuit capacitance $C_{\text{circuit}}=13.9$ fF. The remaining 10.8 fF is photodiode capacitance. Simulations indicate that it is dominated by the capacitance between the p+ region and the nearby channel stop area, by far exceeding depleted region capacitance (Fig. 5). This capacitance can be significantly reduced by careful channel stop design.

Another detector parameter that can be very accurately evaluated by studying X-ray response is interpixel

¹Corresponding author: Gregory Prigozhin, Massachusetts Institute of Technology, Room 37-561, 77 Massachusetts Ave., Cambridge, MA 02139, USA; gyp@space.mit.edu; tel. (617) 253-7246

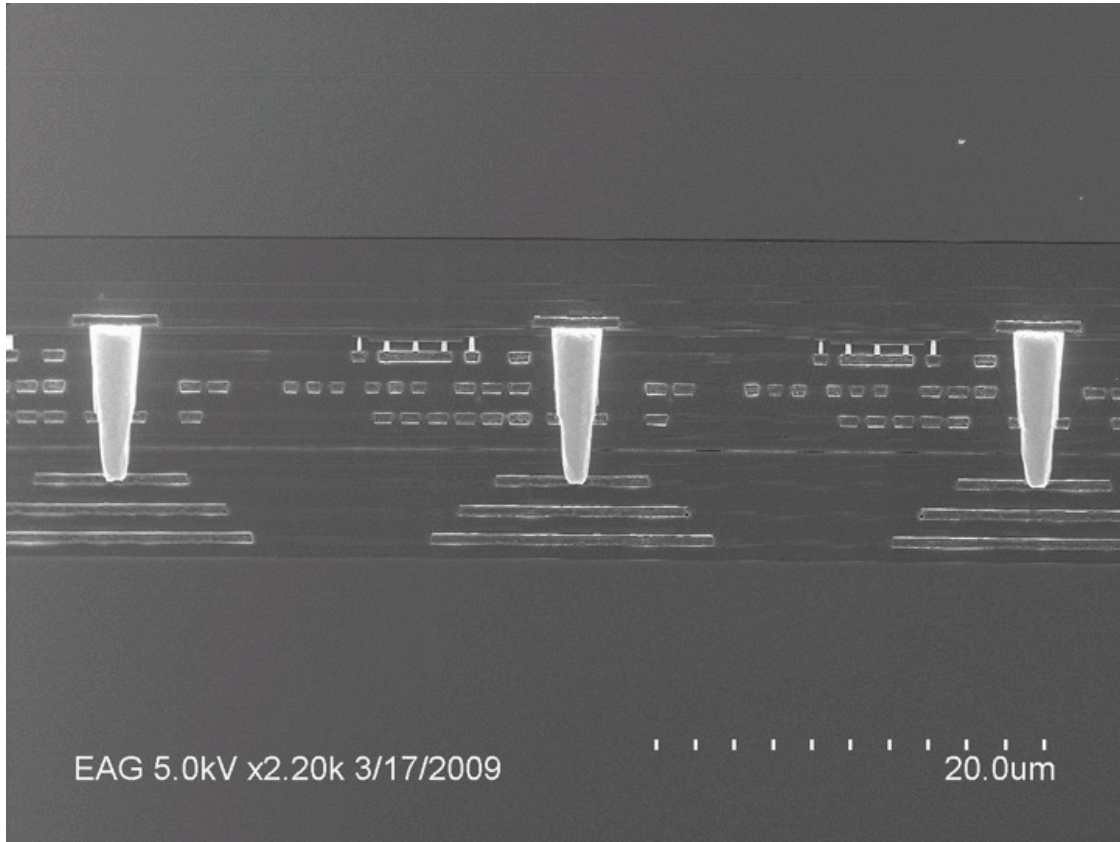


Fig. 1. An SEM photograph of the device cross section. At the bottom part of the 50 micron thick photodiode tier is shown. Tungsten plugs (bright cones) connect it to the SOI circuit.

interaction. Observing signal in the pixels adjacent to the pixel hit by an X-ray photon (see Fig. 6), we were able to measure capacitive crosstalk between pixels. We found that such crosstalk is different in the left and right pixels (0.85% and 8.8% respectively). This crosstalk is caused by the capacitive coupling between the tungsten plug connecting the tiers at the sense node and the output of the source follower in the adjacent pixel. It can be significantly reduced with certain changes in pixel layout. We found that this capacitance, as well as other nearby metal buses, contribute substantially to the sense node capacitance, its reduction can dramatically improve signal/noise ratio.

We have also analyzed contributions of different noise sources by continuously sampling the output with no signal applied to the input in a single-pixel readout mode for a variety of clocking schemes. Performing Fourier transform of the long sequence of readout samples produces noise spectrum of the tested circuit. If the reset gates are held in conductive state, the noise of all the source followers is measured. Not surprisingly, noise spectrum in this case shows a strong $1/f$ component. Taking into account only white noise component, their noise is 15.6 electrons rms at 125 kHz, much higher than expected. Also, noise introduced by clocking reset transistors was determined, results were consistent with calculations based on capacitance values. High noise of the source follower transistors motivated us to measure noise spectra of individual transistors that constitute the SOI readout chain. We found that p-channel transistors having no body ties used in the column source follower have very high noise levels, a factor of 3 higher than similar transistors with body tied to ground in an H-gate layout. This phenomenon is associated with so-called “kink effect” and originates due to impact ionization and accumulation of majority carriers in the transistor body. We also found that transistors after 3D integration exhibit much higher noise levels (approximately by a factor of 3) than the same size transistors before the integration. We have not yet identified with certainty which process step is responsible for such an increase. The next generation sensor will have much lower level of noise once both layout and processing sequence are appropriately modified.

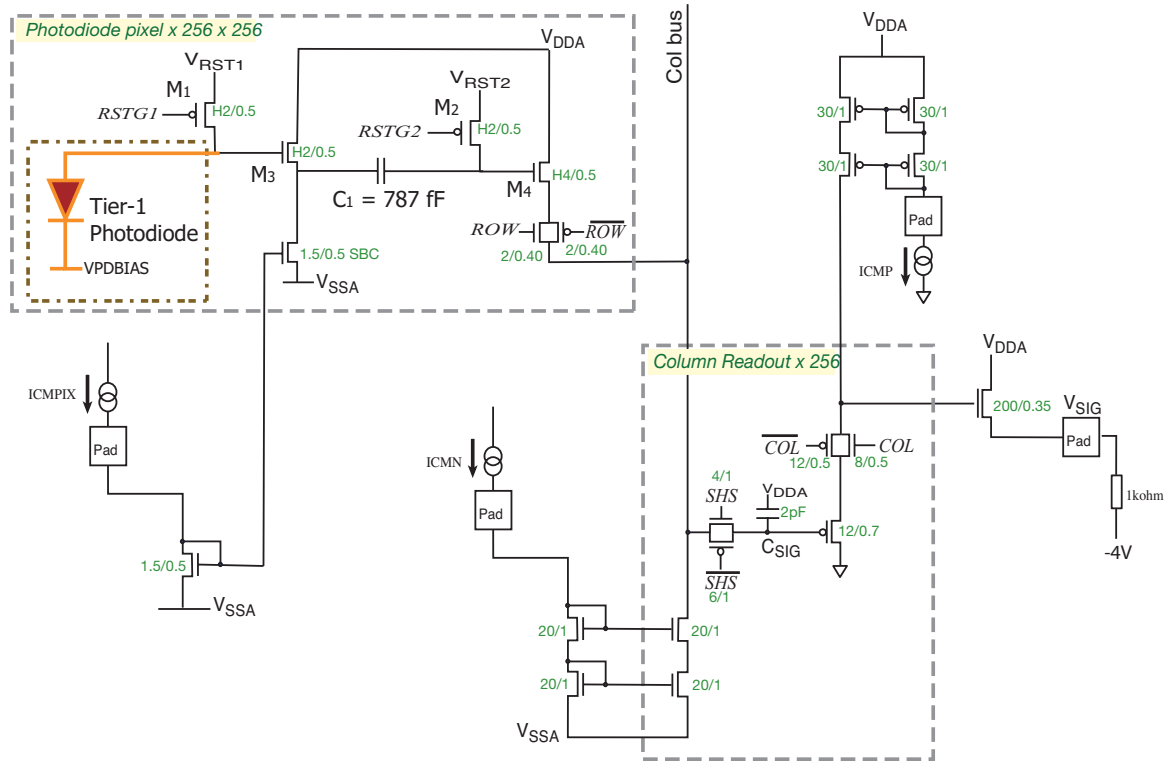


Fig. 2. Device schematic. Only signal readout chain is shown, row and column decoders are omitted.

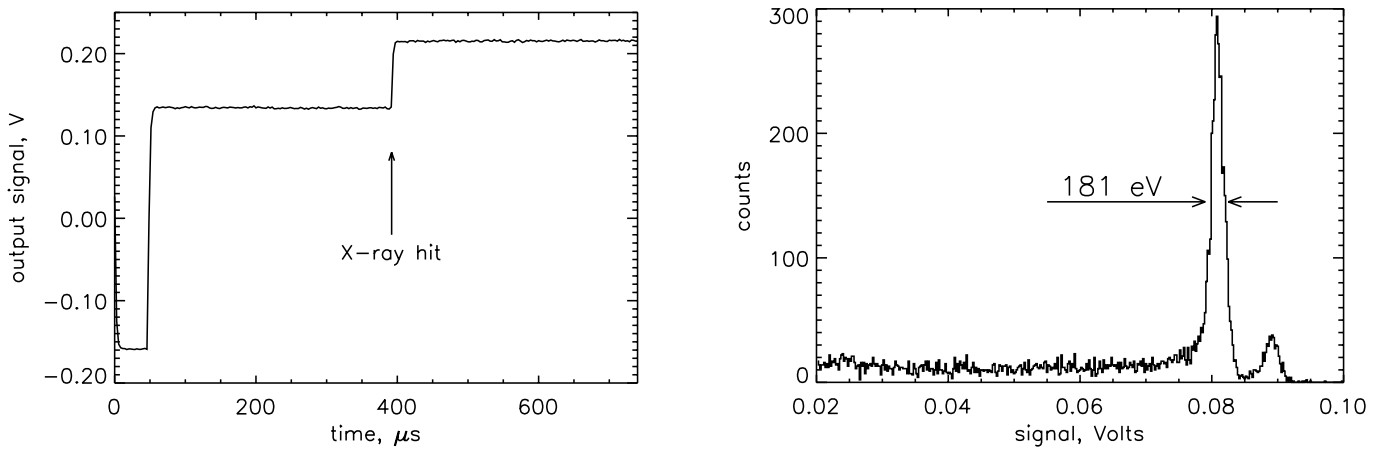


Fig. 3. **Left:** Signal as a function of time in one pixel during repeated sampling after a single reset pulse in the beginning of the line. Device is illuminated by an ^{55}Fe source. Pixel reaction to an X-ray photon hit in the middle of the line is shown. **Right:** A histogram of X-ray events collected by a device illuminated by an ^{55}Fe source. The FWHM of the Mn K_{α} line at 5.89 keV is 181 eV, indicating that charge collection efficiency is very high.

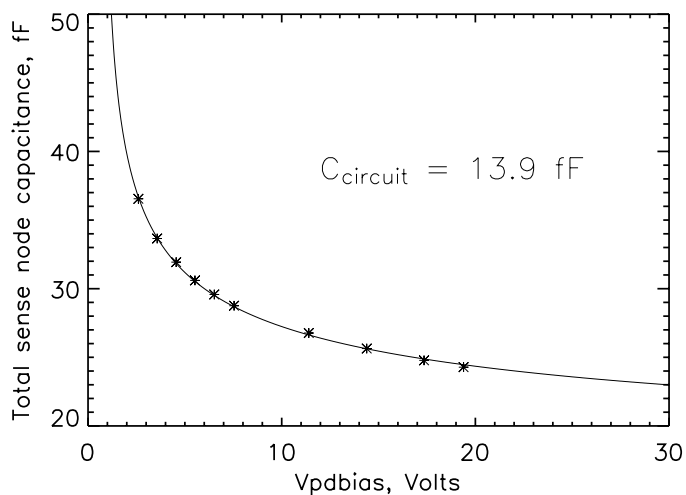


Fig. 4. Sense node capacitance measured with ^{55}Fe X-rays at different voltages applied to the photodiode. Stars indicate experimental data points, solid line is the best fit function describing capacitance of the p-n junction with linearly graded dopant distribution.

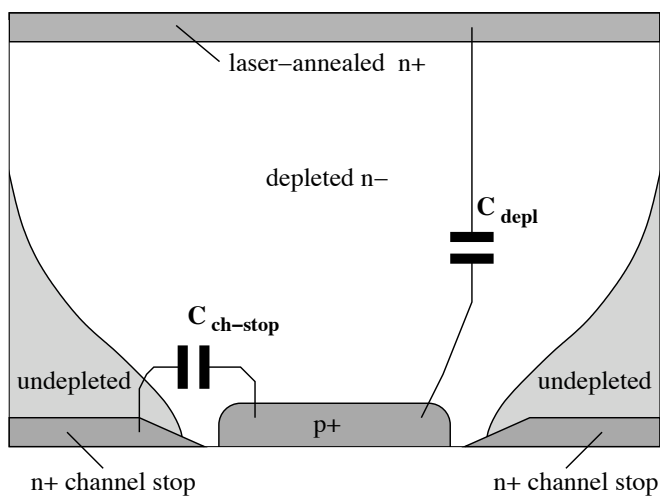


Fig. 5. A cross section of the photodiode tier. The capacitance of the photodiode is dominated by $C_{\text{ch-stop}}$.

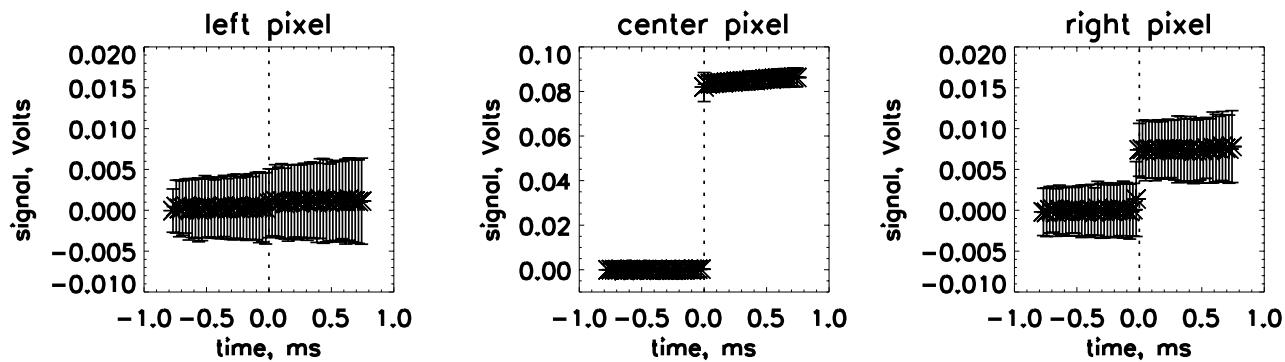


Fig. 6. Averaged signal time profiles in three adjacent pixels corresponding to an X-ray event in the center pixel. Note different vertical scale for pixels on the sides.